SEBHA UNIVERSITY CONFERENCE PROCEEDINGS, VOL.03 NO. 2 2024
DOI: 10.51984/SUCP.V3I2.3104

وقائع مؤتمرات جامعة سبها
Sebha University Conference Proceedings

Confrence Proceeeding homepage: http://www.sebhau.edu.ly/journal/CAS

Investigation on Heat Treated Nickel-Phosphorus (Ni-P) Coating Deposited on the Low Alloy Steel Surface

*Mohammed Al-Kilani Almadani[a], Salah Abdulla Gnefid[b]

[a] Department of Material and Corrosion Engineering, Faculty of Engineering, University of Sebha, Libya.
[b] Mining Department, Natural Resources Faculty, Al-Jufrah University, Libya.

Keywords:
Low Alloy Steels
Ni-P
Electroplating
Heat Treatment
Hardness

ABSTRACT

In the present study, Ni-P composite coating layer has been produced under direct plating condition. The voltage during the experiments has been measured, the results showed that voltage increases with increasing the experiment time. The average applied currents were 0.05 A, 0.08 A and 0.12 A. The employed current densities led to Ni-P rich deposition in all experiments but the average coating thickness was increases with increasing the applied current density. The increasing of electroplating path temperature can also causes increasing in the thickness of Ni-P deposition layer. The best obtained hardness result was at current density of 0.08 A as 285.7 HV. The low alloy steel samples coated by Ni-P deposition layer were heat treated at 400 °C for 1hr causing increasing in microhardness from 270 to about 443.8 HV. XRD analysis showed that Ni-P deposits with 8wt.% are considered as amorphous phase and after heat treatment it was crystallized at steady phases of Ni and Ni_3P deposits.

اختبار طلاء النيكل والفسفور المعالج حرارياً والمترسب على سطح الفولاذ سبيكة الصلب المنخفض

*محمد الكيلاني المدني[1] و صالح عبدالله قنيفيد[2]

[1]قسم هندسة المواد والتآكل، كلية الهندسة، جامعة سبها، ليبيا
[2]قسم هندسة التعدين، كلية الموارد الطبيعية، جامعة الجفرة، ليبيا

الكلمات المفتاحية:
سبائك الصلب المنخفض
التكسية بطلاء النيكل والفسفور
المعالجة الحرارية
الصلادة

الملخص

في هذه الدراسة، تم تغطية سطح سبائك الصلب المنخفض بمركب الفسفور والنيكل بطريقة الترسيب المباشر. تم قياس فرق الجهد خلال التجارب، وأظهرت النتائج أن الجهد يزداد مع زيادة زمن التجربة. لقد وجد أن معدل تكون حبيبات الراسب وحجم الحبيبات للرواسب يعتمدان بشدة على متوسط شدة التيار. وكان شدة التيار المستخدمة 0.05 أمبير و 0.08 أمبير و 0.12 أمبير. أدت شدة التيار المستخدمة إلى ترسيب غني بـ رواسب الفسفور والنيكل في جميع التجارب ولكن متوسط سمك الراسب يزداد مع زيادة شدة التيار المستخدم. يمكن أن تؤدي زيادة درجة حرارة محلول الترسيب الكهربائي أيضًا إلى زيادة سمك رواسب الفسفور والنيكل. أفضل صلادة لسبائك الصلب المنخفض المغطى بطبقة من رواسب الفسفور والنيكل تم الحصول عليها عند شدة التيار 0.08 أمبير وكانت 285.7HV. تمت معالجة عينات سبائك الصلب المنخفض المطلية برواسب الفسفور والنيكل بالحرارة عند 400 درجة مئوية لمدة ساعة واحدة حيث أدى ذلك إلى زيادة الصلادة إلى حوالي 443.8 HV, وكان معدل الزيادة حوالي 35.62%. أظهر تحليل حيود الأشعة السينية (XRD) أن رواسب الفسفور والنيكل بنسبة 8% من الوزن تعتبر طورًا غير متبلور وبعد المعالجة الحرارية تم تبلورها في أطوار ثابتة من رواسب النيكل وفوسفيد النيكل الثلاثي(Ni_3P).

*Corresponding author:
E-mail addresses: moh.ibrahim@sebhau.edu.ly, (S. A. Gnefid) s.gnefid@gmail.com
Article History : Received 15 April 2024 - Received in revised form 14 September 2024 - Accepted 6 October 2024

1. Introduction

Most often utilized structural materials are low-alloy steels, which have an alloying element content of 4% or less. For a wide range of technical applications, these materials are very appealing due to their inexpensive price and good mechanical performance following suitable heat treatment. [1]. Another name for AISI 4140 alloy is "chrome-moly" steel. 4140 alloy is strong, ductile, and wear resistant, making it perfect for forging and heat treatment. The highest possible Rockwell hardness range is C20–C25. It melts at 1510 °C [2]. The majority of industry sectors make substantial use of AISI 4140 alloy steel for a variety of applications, including pump shafts, bolts, crankshafts, and hydraulic shafts and parts [3]. AISA 4140 can be heat treated in a variety of ways to provide the benefits of appropriate hardness, strength, and ductility all at once [4]. Numerous methods, including mechanical, physical, chemical, and electrochemical ones, are available for coating deposition [5]. Among these, basic electroplating has several benefits. It is a low-cost electrolysis cell technique that operates in an aqueous solution at room temperature, normal pressure, and relatively low temperature, making it perfect for industrial scaling up [6-7-8]. Ni-P alloy electrodeposits are mostly used in the automotive, aerospace, and general engineering industries as protective, functional, and ornamental coatings [9]. Applications of Ni-P in the production of high precision parts, diffusion barriers, catalytic coatings for hydrogen evolution, thin film magnetic discs, micro-galvanic, and decorative coatings for the automobile industry are noteworthy [9]. The current study set out to examine how heat treatment affected the Ni-P alloy coating that was applied to the surface of plain carbon steel using an electrodeposition technique. Additionally, various current densities were used to determine how they affected the average thickness of the Ni-P deposit. Lastly, the impact of heat treatment on the resulting microstructure phase was determined by XRD analysis.

2. Literature Review

In (2022), M. S. Senthil Saravanan, et. al., [10], studied the properties evaluation of electroless Ni-P coated low-carbon steels. The purpose was to determine how long a heat treatment process had on the mechanical and corrosion performances of a Ni-P coating on low-carbon steel. The coating is performed on the low-carbon steel using Ni-P salt bath. The coated samples were heat treated at (400 °C) under atmospheric condition using muffle furnace. The heat treatment offers greater corrosion resistance and mechanical qualities. The coated samples were analyzed using scanning electron microscope for morphological studies and X-ray diffraction analysis for phase change during heat treatment. According to the experimental findings, a heat treatment prior to coating with Ni-P layer increases hardness and corrosion resistance while lowering friction.

In (2021), F. Lekmine, et. al., [11], studied the effects of current density on Ni–P coating obtained by electrodeposition. In this work, Ni–P coatings are deposited on the steel substrate by electrodeposition from a solution containing nickel sulfate and sodium hypophosphite (NaH_2PO_2). The effect of the current density on the morphology, phase structure, microhardness, and corrosion performance of the Ni–P coatings are studied. Scanning electron microscopy and energy dispersive (X-ray) analysis and (X-ray) diffraction are used to study the morphological, composition and phase structure. The corrosion performance of the coatings is evaluated by weight loss, electrochemical impedance spectroscopy and Tafel polarization. Results showed that the morphology of the electrodeposited Ni–P alloys coatings has spherical grains for all the samples, and the (Ni_3P) phases are formed all over the microstructure of the coatings. It is observed that the phosphorus content and microhardness are dependent on the current density. The corrosion tests show that (5 Adm^{-2}) current density is the optimal value which gives the best protective coating against corrosion. It also exhibits superior microhardness originated from the higher (Ni_3P) amount.

In (2020), F. Lekmine, et. al., [12], investigated the mechanical characterization of electrodeposition of Ni-P alloy coating. In this study, Ni-P coatings were deposited on (X52) steel substrates by electrodeposition technique from a solution containing nickel sulfate, sodium hypophosphite (NaH_2PO_2). Composition, surface morphology, and mechanical properties of the Ni-P deposits were studied using (SEM), (EDAX), the Vickers method, weight loss and potentiodynamic polarization techniques. The effects of the current density were investigated on the surface morphology, phosphorus content, microhardness and corrosion of the coatings. It was observed that both the phosphorus content and microhardness are dependent on the current density. Results demonstrate that the morphology of the electrodeposited Ni-P alloys shows that the grains are spherical in nature for all the samples. It has been observed that the influence of current density on the P content of the deposit is an inverse relation with phosphorous content and also the as-plated coatings at current density of (5 Am^{-4}) exhibit the superior microhardness. Corrosion tests show that (5Am^{-4}) is the best current density value which gives the best protection coating against corrosion.

3. Experimental Details

3.1 Ni-P Electrodeposition Experiments Apparatus

The system employed in this work for direct current electrodeposition of Ni-P deposits is shown schematically in Figure (3.1). The main components of this system are: (i) A power supply (Model PAD, (0~35 Volts, 20 Amperes); (ii) 250ml beaker was used in this study; (iii) Bath temperature controller; (iv) Heater (Model REXIM RSH – 1D); (v) (3.5 cm x 1.4 cm x 0.15 cm; AISI 4140 low alloy steel samples), (0.4 C, 0.88 Mn, 0.95 Cr, 0.2 Mo and Fe balance) wt. % [13], one face of the cathode was only exposed to the electrolyte. The cathode was connected to the positive side of the power supply; (vi) Anode (Graphite 10 cm x 2.5 cm x 0.4 cm), the surface area of anode approximately six times greater than that of cathode: (vii) Voltameter/Ammeter (Model FLUKE 75 MULTETER); (viii) Magnetic stirrer (stirring velocity was 300 rpm for all deposition sessions); (ix) Anode/Cathode holders (Copper rod holders). A modified watt-baths were used to electrodeposit Ni-P deposit. and the temperature of the baths were (60 °C and 70 °C). Before each deposition session, the steel cathode surface was mechanically cleaned and polished to achieve mirror-finish surface.

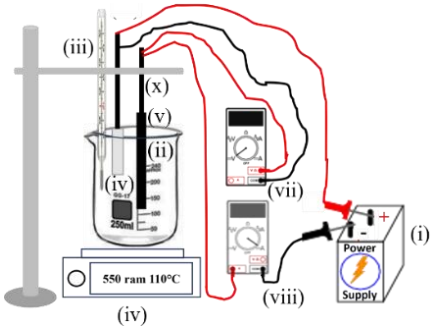

Fig. 1: A Schematic of Ni-P Deposition Cell Used in this Work.

3.2 Ni-P Electroplating Bath

Table (1) shows the baseline chemicals and their composition of the first bath employed in Ni-P electrodeposition experiments.

Table 1: The Baseline Chemicals and their Composition of the First Bath Employed in Ni-P Electrodeposition Experiments.

Dissolved Substance	Chemical Formula	Purity %	Mol. Wt. (g/mol)	Concentration in Bath (g/L)
Nickel Sulfate	$NiSO_46H_2O$	99	262.845	150
Nickel Chloride	$NiCl_26H_2O$	99	237.690	45
Sodium Hypophosphate	$NaH_2PO_2H_2O$	100	105.970	50
Boric Acid	H_3BO_3	99.5	061.811	50

3.3 Ni-P Electroplating Bath

(i) Prepare the required weight of each salt and acid; (ii) The salts and acids are added one by one to 75 mL, distillated water (pH 5); (iii) Temperature during salt mixing process was (60°C-80°C); (iv) Stirring velocity during mixing was (300 rpm); (v) Mixing time (1 hr); (vi) The bath solution was poured into a volumetric flask (200 mL); (vii) Distillate water was added to adjust (200 mL) volume.

3.4 Ni-P Electrode Electrodeposition Preparation

(i) Five low alloy steel plates (3.5cmx1.4cmx0.15cm) were abrasive polished No. (400 AGP, 800 AGP, 1000 AGP, 1500 AGP, 2000 AGP, 6 µm AGP and 1 µm AGP) respectively; (ii) Rinsing using distillated water, then drying; (iii) Ultrasonic cleaning using alcohol solution for

(1 min) period time; (iv) (6 µm) polishing using diamond paste lubricated by kerosene; (v) Soap washing followed by rinsing, then drying; (vi) Ultrasonic cleaning using alcohol solution for (1 min) period time; (vii) (1 µm) polishing using diamond paste lubricated by kerosene; (viii) Soap washing followed by rinsing, then drying; (ix) The cathode immersed in solution hydroxide for (30 m 9n); (x) The cathode immersed in pickling diluted (HCl) solution for (60 seconds); (xi) Graphite anode surface was polished using abrasive paper in order to get smooth surface. Figure (2) showing the plain carbon steel plate (cathode) before surface preparation and the stages of low alloy steel plate preparation for Ni-P electroplating.

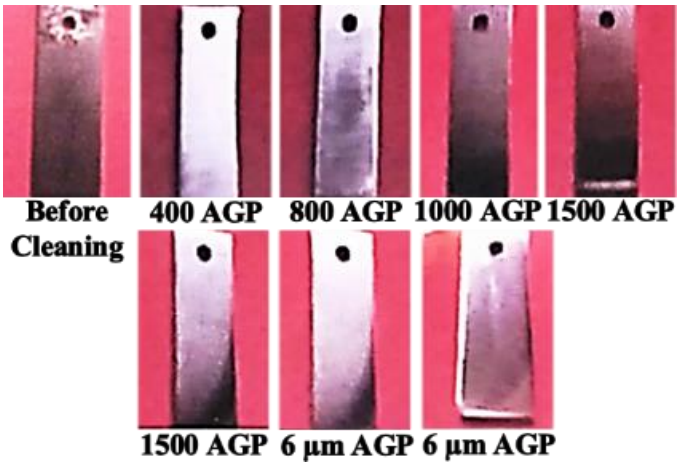

Fig. 2: The AIAI 4140 Low Alloy Steel Plate (Cathode) before Surface Preparation and the Stages of AISI 4140 Low Alloy Steel Plate Preparation Using AGP for Ni-P Electroplating.

3.5 Ni-P Electroplating Experiment Steps

(i) The electroplating cell was connected as shown in Figure (3.1); (ii) The electroplating path temperature was adjusted; (iii) The electroplating path pH was measured; (iv) The current from the rectifier was switched on; (v) To avoid contamination with carbon produced by the graphite anode, the anode surface was covered with filtration paper prior to immersed into the path solution; (vi) The anode-cathode distance adjusted doe (3 cm); (vii) Voltage was measured periodically after (10 min, 20 min, 30 min, 40 min, 50 min and 60 min); (viii) After the electroplating process has finished: (a) The electroplated low alloy steel sample was washed with soap, followed by rinsing with distillated water; (b) The sample then weighted; (c) The weight of deposited Ni-P was calculated.

3.6 Sample Preparation to Measure the Average Thickness of Ni-P Deposit

(i) Sectioning: At the middle of the low alloy steel plate, a small area (1.4 cm x 1.0cm) was cut; (ii) Cold Mounting: The small sample size was embedded in epoxy material type; (iii) Grinding: In order to remove the damage on the sample surface, an abrasive grit paper was used; (iv) Polishing: In order to produce a smoot sample surface, different types of an abrasive grit papers were used (120, 320, 400, 800, 1500 and 2000) respectively. Figure (3) showing the steps of sample preparation to measure the Ni-P deposition layer on the carbon steel plate.

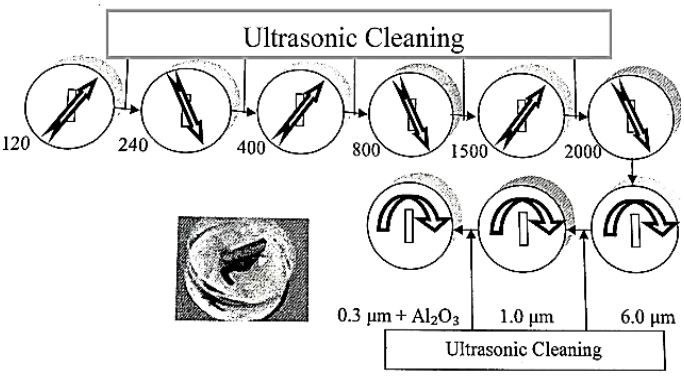

Fig. 3: The Steps of Sample Preparation to Measure the Ni-P deposition layer on the Low Alloy Steel Plate.

3.7 Heat Treatment of Plain Carbon Steel Samples Coated with Ni-P Deposit

3.7.1 Sample Preparation Prior to Heat Treatment Process

(i) Sample was ultrasonic cleaned followed by rinsing then drying; (ii) The sample was covered with aluminum foil in order to avoid any oxidation during heat treatment; (iii) The sample was preheated prior to heat treatment process.

3.7.2 Heat Treatment Procedure

(i) The sample was put in furnace crucible; (ii) Argon gas was pumped continuously until it was confirmed that all gases inside the furnace had been expelled; (iii) The furnace was turned on, and its temperature was set at (400 °C); (iv) The gradually increasing of the furnace temperature was monitored; (v) When the furnace temperature reached (400°C), the crucible containing the sample was placed inside the furnace and left inside the oven for a full hour; (vi) The furnace was turned off and left it to cool until the temperature reached (300°C); (vii) The sample was taken out of the furnace and left to cool in atmospheric air; (viii) Sample was ultrasonic cleaned followed by rinsing then drying. Figure (4) showing the schematic sketch of ceramics heat Treatment furnace.

3.8 Ni-P Deposition layer Hardness Test

The electrodeposited low alloy steel plates were cold mounted, then polished to finish-mirror followed by ultrasonic cleaned for (1 min). Because of the average thickness of Ni-P deposits was thin (few microns), the hardness was characterized by a microhardness indention method. The hardness tests were carried out by Vicker Hardness Tester (LECO, DM-400) with a load of (50 g). Load (F) applied perpendicular to the smooth free surface of the Ni-P deposit.

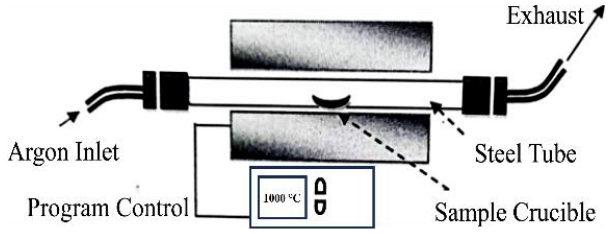

Fig. 4: A Schematic Sketch of Ceramics Heat Treatment Furnace.

4. Obtained Results

4.1 Ni-P Electrodeposition Operating Conditions:

4.1.1 Ni-P Electrodeposition Experiments Operating Conditions:

Table (2) shows the operating conditions for the Ni-P electrodeposition experiments (1.1, 1.2, 1.3, 2.1, 2.2 and 2.3).

Table 2: The Operating Conditions for the Ni-P Electrodeposition Experiments (1.1, 1.2, 1.3, 2.1, 2.2 and 2.3).

Experiment No.	Applied Current (A)	Bath Temp. (°C)	Experiment Duration Time (min)
1.1	1.20	70	136
1.2	1.90	70	85
1.3	2.86	70	60
2.1	1.20	60	136
2.2	1.90	60	85
2.3	2.86	60	60

4.1.2. Ni-P Electrodeposition Experiments Voltage Registration:

Table (3) showing the voltage registration for each (10 min) of the Ni-P electrodeposition experiments (1.1, 1.2, 1.3, 2.1, 2.2 and 2.3).

4.2 Average Thickness of Ni-P Deposit:

The averages thickness of the Ni-P deposition layer coated on the surface of low alloy steel plate were listed in Table (4). Figure (5.1) and (5.2) showing the Ni-P deposits on the surface of low alloy steel plate photos for experiments (1.1, 1.2, and 1.3) and experiments (2.1, 2.2 and 2.3) respectively under microscope (500 X) magnification.

4.3 Hardness Measurements Prior and After Heat Treatment:

Table (4.4) Showing the microhardness measurements average prior and after heat treatment process. Figure (6) showing the comparison between the microhardness measurements prior and after the heat treatment of the low alloy steel samples coated by Ni-P deposits.

Table 3: The Voltage Registration for Each (10 min) of the Ni-P Electrodeposition Experiments (1.1, 1.2, 1.3, 2.1, 2.2 and 2.3).

Interval Time (min)	Voltage Registration (volt)					
	Ni-P Electrodeposition Experiment No.					
	1.1	1.2	1.3	2.1	2.2	2.3
0	0.758	1.846	0.979	0.965	0.980	1.531
10	0.980	1.850	1.610	1.691	1.469	1.944
20	1.141	1.865	1.765	1.802	1.619	1.924
30	1.533	1.885	1.884	1.846	1.740	1.929
40	1.614	1.636	1.924	1.836	1.332	1.783
50	1.616	1.673	1.930	1.843	1.375	1.743
60	1.644	1.782	1.852	1.842	1.386	1.737
70	1.615	1.850	-	1.881	1.406	-
80	1.462	1.856	-	1.888	1.606	-
90	1.655	-	-	1.8857	1.720	-
100	1.650	-	-	1.862	-	-
110	1.723	-	-	1.879	-	-
120	1.696	-	-	1.893	-	-
130	1.710	-	-	1.851	-	-
136	1.790	-	-	1.868	-	-

4.4 Ni-P Deposition layer Cross-Section and Composition Determination:

The chemical composition of heat treated the plain carbon steel samples coated by Ni-P deposits was determined by energy dispersive specimen (EDS) using (SEM) with a (Nouran) instruments microanalysis system. The results of chemical composition were taken under a (SEM) at (500X) magnification. Figures (7a), (7b), (7c), (7d), (7e) and (7f) showing (SEM) micrograph cross-section of deposits by modified watt-bath at (1.90 A/dm², 60 °C), (2.86 A/dm², 60 °C), (1.20 A/dm², 60 °C), (1.90 A/dm², 70 °C), (2.86 A/dm², 70 °C), and (1.20 A/dm², 70 °C) respectively. Table (5) listed the (%) average phosphor and nickel contents in Ni-P deposits.

4.5 Identification of the Chemical Composition of AISI 4140 Low Alloy Steel Used as A Cathode in the Present Work:

The chemical composition of plain carbon steel used in the present work was identified using (SEM) at (500X) magnification. The types of main elements and their compositions of chemical composition are listed in Table (7). Figure (8) shows the (SEM) results of the plain carbon steel used in the present work.

Table 4: The Ni-P Deposition layer Averages Thickness.

Experiment No.	Applied Current (A)	Ni-P Deposit Averages Thickness (µm)
1.1	1.20	33.42
1.2	1.90	39.69
1.3	2.86	56.69
2.1	1.20	29.02
2.2	1.90	39.79
2.3	2.86	44.16

Table 5: The Microhardness Measurements Average Prior and After Heat Treatment Process.

Experiment No.	Average Microhardness (HV)		Microhardness Increasing After Heat Treatment (%)
	Prior to Heat Treatment	After Heat Treatment	
1.1	270.0	419.1	35.58
1.2	285.7	425.3	32.82
1.3	253.2	416.5	39.21
2.1	260.0	442.6	41.13
2.2	275.4	431.6	36.19
2.3	270.7	443.8	39.00
	Average		37.32

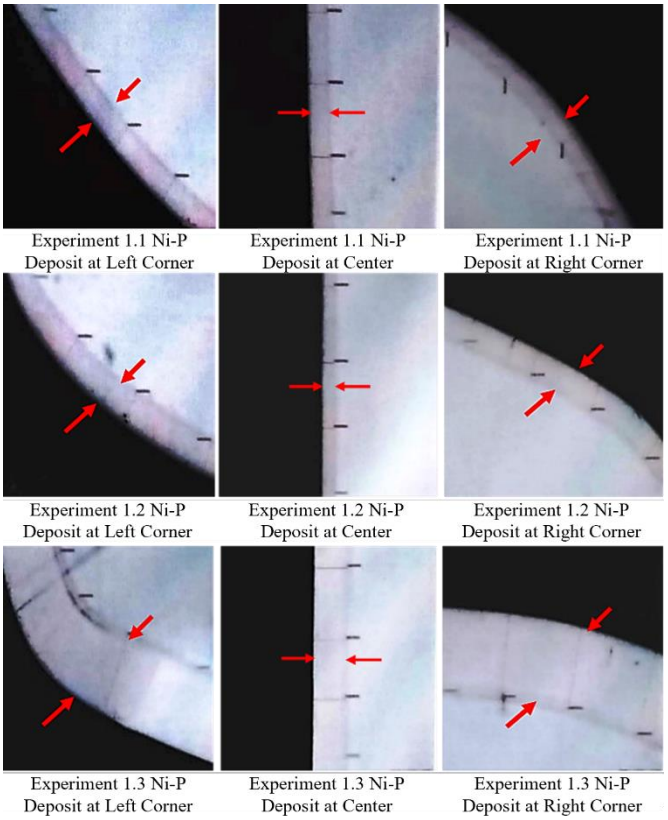

Fig. 5.1: The Ni-P Deposits on the Low Alloy Steel Surface of Experiments (1.1, 1.2, and 1.3) (Microscope 500 X Magnification).

3.6 Identification the Ni-P Deposits Using (XRD):

To identify the phases of the Ni-P deposits, one sample (the experiment 2.1) was selected for testing with XRD machine.

3.6.1 Anchor Scan Parameters:

The Anchor scan parameters for the Ni-P deposits (XRD) of the experiment (2.1) are listed in Table (7).

3.7 (XRD) Peak List and Graphic:

The Ni-P deposit (XRD) peak list of the experiment (2.1) is listed in Table (4.7) and the (XRD) graphic patterns before and after heat treatment process are shown in Figure (9) and (10).

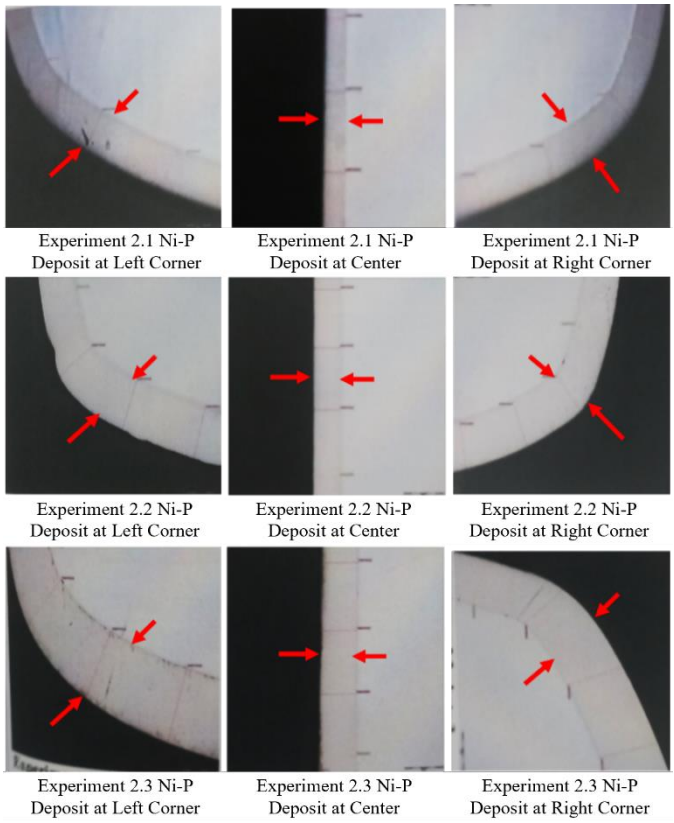

Fig. 5.2: The Ni-P Deposits on the Low Alloy Surface of Experiments (2.1, 2.2, and 2.3) (Microscope 500 X Magnification).

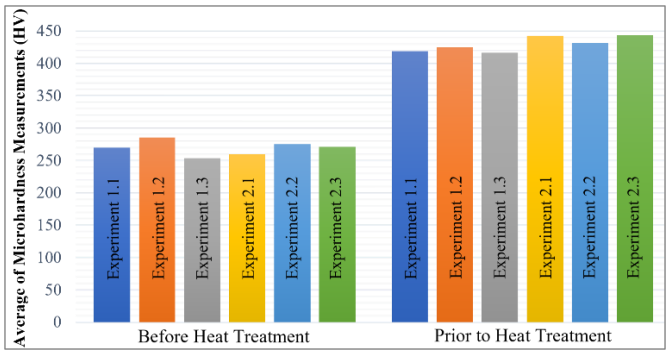

Fig. 6: The comparison Between the Microhardness Measurements Prior and After the Heat Treatment of the Low Alloy Steel Samples Coated by Ni-P Deposit.

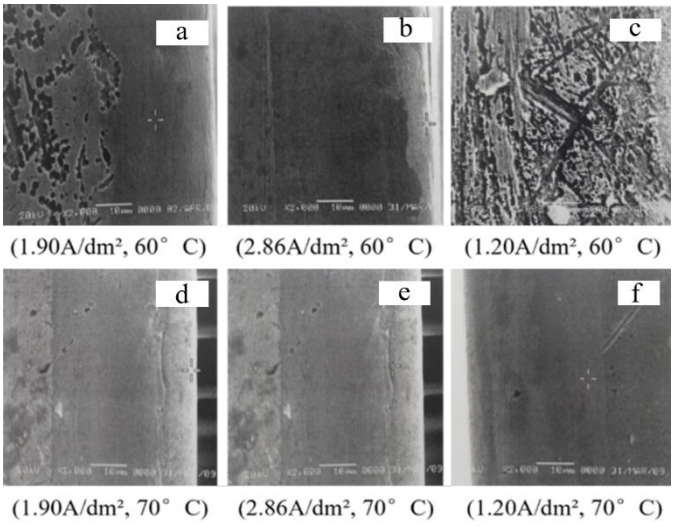

Fig. 7a, b, c, d, e and f: (SEM) Micrograph Cross-Section of Deposits by Modified Watt-Bath

Table 6: (%) of Phosphor and Nickel Contents in Ni-P Deposits.

Experiment No.	Average Mass Fraction of Phosphor in Ni-P Deposit (%)	Average Mass Fraction of Nickel in Ni-P Deposit (%)
1.1	13.97	86.03
1.2	12.33	87.67
1.3	09.50	90.50
2.1	14.88	85.12
2.2	13.78	86.22
2.3	12.44	87.56

Table 7: AISI 4140 Low Alloy Steel Chemical Composition.

Element	Chemical Symbol	Chemical Composition Mass (%)
Carbon	C	00.40
Manganese	Mn	00.88
Chromium	Cr	00.95
Molybdenum	Mo	00.20
Iron	Fe	95.50

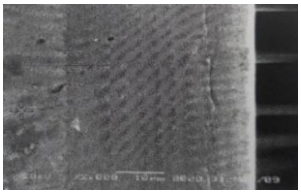

Fig. 8: AISI 4140 Low Alloy Steel (SEM) Micrograph.

Table 8: The Anchor Scan Parameters for the Ni-P Deposits (XRD) of the Experiment (2.1).

Dataset Name	Experiment (2.1)
Start Position [°2Th.]	20.010
End Position [°2Th.]	89.990
Step Size [°2Th.]	00.020
Scan Step Time [a]	00.500
Divergence Slit Type	Fixed
Specimen Length [mm]	10.000
Measurement Temperature [°C]	25.000
Anode Material	Cu
k-Alpha [°A]	01.54056
Generator Setting	30mA, 40mA

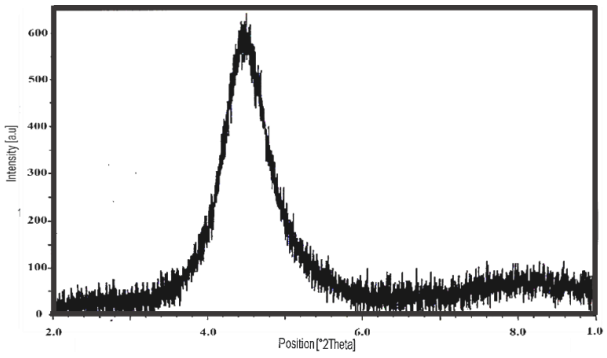

Fig. 9: The Ni-P (XRD) Graphic Patterns of the Experiment (2.1) (After Heat Treatment Process).

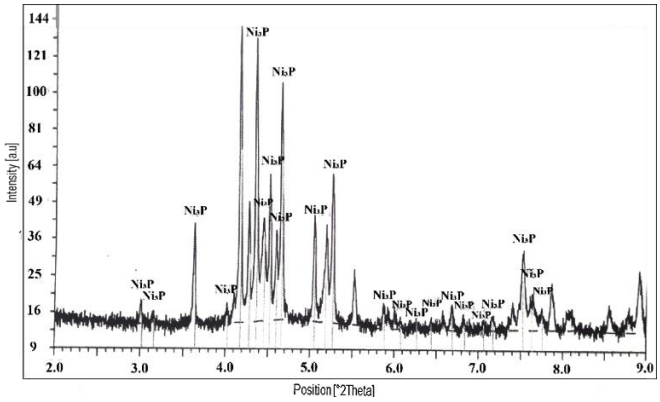

Fig. 10: The Ni-P (XRD) Graphic Patterns of the Experiment (2.1) (Before Heat Treatment Process).

Table 9: Peak List Ni-P Deposit of the Experiment (2.1).

Position [°2Th.]	Peak Intensity Counts	d-Spacing [°A]	Rel. Intensity [%]	Peak Width [°2Th.]
23.100	20	3.8567	1.0	0.320
30.090	58	2.9748	4.0	0.120
31.450	38	2.8492	1.8	0.240
36.235	552	2.4832	26.3	0.160
40.085	69	2.2532	3.3	0.120
40.970	117	2.2065	5.6	0.120
41.575	2098	2.1758	100.0	0.220
42.665	625	2.1227	29.8	0.100
43.465	2034	2.0855	97.0	0.140
43.465	1640	2.0809	78.2	0.060
44.380	458	2.0446	21.8	0.240
45.120	762	2.0128	36.3	0.200
45.855	388	1.8922	18.5	0.100
46.510	1406	1.9558	67.0	0.200
50.425	424	1.8128	20.2	0.100
51.860	384	1.7659	18.3	0.060
52.550	600	1.7444	28.6	0.180
55.220	161	1.6662	7.7	0.240
58.715	61	1.5751	2.9	0.160
60.060	49	1.5430	2.3	0.120
64.385	16	1.4494	0.8	0.320
65.870	26	1.4203	1.2	0.320
66.860	52	1.4017	2.5	0.240
68.270	18	1.3761	0.9	0.240
71.725	19	1.3181	1.4	0.320
74.100	55	1.2816	2.6	0.200
75.245	196	1.2649	9	0.320
76.570	71	1.2463	3.4	0.160
77.580	42	1.2326	2.0	0.160
78.705	96	1.2178	4.6	0.200
80.995	32	1.1891	1.5	0.480
85.535	44	1.1372	2.1	0.200
87.905	32	1.1126	1.5	0.320
89.060	121	1.1011	5.8	0.120

5. Results Discussion:

5.1 Anode-Cathode Voltage

The voltage measurements showed that the voltage increases with increasing the Ni-P electrodeposition experiment time, after approximately (30 min), the voltage either increases slightly or remain constant, this attributed to the increasing of the electrolyte resistance according to the Ohm's Law of Voltage (Voltage = Current Density/Resistance) [13]. As listed in Table (3), the suddenly decreases in the voltage is attributed to the presence of the impurities in electrolyte.

5.2 Cathodic Current Density

The nucleation rate and hence the grain size of electrodeposition has been found to be strongly dependent upon the average plating current density. The employed current densities in this work led to Ni-P rich deposition in the whole of performed experiments, but the Ni-P deposit average thickness was varied and highly related with the applied current density. The Ni-P average deposit thickness increases with increasing of the applied current. The Ni-P deposit averages thicknesses in this works deposition experiments were ranged from (33μm to 56μm).

5.3 Electrolyte Bath Temperature

As the temperature of the electrodeposition electrolyte was maintained at (70 °C), the Ni-P deposit average thickness increases sharply with increasing the current density, while at (60 °C), the increase in Ni-P deposit average thickness was less comparing with (70 °C), this was attributed to the decreasing of the cathodic current density. Thus, the increasing in electrolyte bath temperature during electrodeposition process leads to more average thickness of the deposit.

5.4 Effect of Heat Treatment on Microhardness of Ni-P Deposit:

Figure (6) showed that the microhardness of the crystalline structure of Ni-P deposit (after heat treatment process) is much greater than that of the amorphous Ni-P deposit. After heat treatment, the average increasing of the Ni-P microhardness was about (37%).

5.5 Phase Identification

(XRD) patterns of Ni-P deposit before and after the heat treatment process according to the Figures (9) and (10) respectively, indicating that the Ni-P deposit before heat treatment process consisted of an amorphous nickel, that was illustrated on the Figure (9) with no peaks were considered. After the heat treatment takes place, the new additional pattern peaks (Ni_3P-phase) as on Figure (10) were performed, which reflected that the Ni-P phase was transformed from amorphous to crystalline structure. A similar phenomenon of crystallization of metastable Ni-P into a stable (Ni_3P - phase) has been reported in references (14, 15 and 16).

6. Conclusions

In this work, direct electrodeposition was used to create the Ni-P deposits on the surface of low alloy steel plates at various current densities and temperatures. The electrolyte bath used for electrodeposition was made up of boric acid, sodium hypophosphate, nickel chloride, and nickel sulphate. These approaches were effective for examining how heat treatment affected the Ni-P deposits' increased microhardness. Based on the findings, the following conclusions can be made:

(i) The voltage increases with increasing the Ni-P electrodeposition experiment time;

(ii) The Ni-P deposition layer average thickness increases with increasing of the applied current;

(iii) The increasing in electrolyte bath temperature during Ni-P direct electrodeposition process leads to more average thickness of the deposit.

(iv) The microhardness of the crystalline structure of Ni-P deposit (after heat treatment process) is much greater than that of the amorphous Ni-P deposit. After heat treatment process, the average increasing of the Ni-P microhardness was about (37%).

References

[1]- Goodwin, F., et. al., (2005), In Springer Handbook of Condensed Matter and Materials Data; *Warlimont, H. Metals; Martienssen, W., Warlimont, H., Eds.; Springer: Berlin, Germany, pp. 161–430*.

[2]- Xiong, Z., et. al., Clustering, (2021), Nano-Scale Precipitation and Strengthening of Steels. *Prog. Mater. Sci., 118, 100764*.

[3]- McMaster-Carr Supply Company, (2003), Steel Grades and Their Properties, A Special Supplier of Machines, Tools, Raw Materials, Industrial Materials and Maintenance Equipment, Elmhurst, Illinois, United States.

[4]- AC Manufacturing, (2017), Highest Quality Manufacturing and Machining Services, *Unit 5, 10B Stadium Business Park, Ballycoolin Road, Dublin 11, D11 CKN7, Irland*.

[5]- P. SIDKY and M. HOCKING. "Review of Inorganic Coatings and Coating Processes for Reducing Wear and Corrosion". In: *British Corrosion Journal 34.3 (1999), pp. 171–183. DOI: 10.1179/000705999101500815 (cit. on pp. 1, 2).*

[6]- M. SCHLESINGER and M. PAUNOVIC, (2011) eds. Modern Electroplating: Fifth Edition. John Wiley & Sons, Inc., *DOI: 10.1002/9780470602638 (cit. on pp. 1, 2, 11, 12).*

[7]- N. KANANI. Electroplating. Elsevier, (2004), *DOI:10.1016/B978-1-85617-451-0.X5000-3 (cit. on p. 1).*

[8]- F. NASIRPOURI. Electrodeposition of Nanostructured Materials. Springer, (2017), p. 325. DOI: 10.1007/978-3-319-44920-3 (cit. on p. 1).

[9]- T. W. Scharf and S. V. Prasad, (2013), "Solid lubricants: A review". *In: Journal of Materials Science 48.2, pp. 511–531. DOI: 10.1007/s10853-012-7038-2 (cit. on p. 2).*

[10]- M. S. Senthil Saravanan, et. al., (2022), Properties Evaluation of Electroless Ni-Coated Low-Carbon Steels, Journal of Nanomaterials, *Research Article, Open Access, Volume 2022, Article ID: 8497927 https://doi.org/10.1155/2022/8497927*.

[11]- F. Lekmine, et. al., (2021), Effects of Current Density on Ni–P Coating Obtained by Electrodeposition, Physics Department, ABBES Laghrour Khenchela University, P.O. 1252, 40004, Algeria, *Metallophysics and Advanced Technologies Metallofiz. Noveishie Tekhnol, 2021, vol. 43, No. 10, pp. 1351–1363, https://doi.org/10.15407/mfint.43.10.1351*.

[12]- F. Lekmine, et. al., (2021), Mechanical Characterization of Electrodeposition of Ni-P Alloy Coating, Physics Department, ABBES Laghrour Khenchela University, P.O. 1252, 40004, Algeria, *Journal of Nano and Electronic Physics, Vol. 12 No 1, 01001(5pp). DOI: 10.21272/jnep.12(1).01001 PACS numbers: 68.37.– d, 68.37.– Ps, 81.65.– b, 81.65.– Cf.*

[13]- INCO, (2021), Composition of Alloy Steels, A Practical Guide to the Use of Nickel-Containing Alloys, No. 447, Distributed by: Nicke Institute,

https://nickelinstitute.org/media/8d91b9f21353d5f/ni_inco_447_compositionsofalloysteels.pdf.

[14]- Mohan Bahadur Basnet, (2023), Ohm's Law, Gauhati University, Parliament, Pratinidhi Sabha Guwahati 781014, Assam, India, *Researchgate*, *https://www.researchgate.net/publication/370051437_Ohm's_Law*.

[15]- G. Straffelini, D. Colombo, and A. Molinair, (1999), Surface Durability of Electroless Ni–P Composite Deposits, Department of Materials Engineering, University of Trento, via Mesiano 77, 38050 Trento, Italy Sincedirect, https://doi.org/10.1016/S0043-1648(99)00273-2.

[16]- K Uday Venkat Kiran, et. Al., (2019), Sliding Wear Characteristics of as-Deposited and Heat-Treated Electroless Ni-P Coatings Against AISI E52100 Steel Ball, Materials Research Express, Volume 6, Number 3, DOI 10.1088/2053-1591/aaf2f9, https://iopscience.iop.org/article/10.1088/2053-1591/aaf2f9/pdf.

[17]- Aleksandra Lelevic, et. Al., (2019), Electrodeposition of Ni-P alloy coatings: A Review, Artia Nanoengineering & Consulting, Athens, Greece, *Sincedirect, Volume 369, https://doi.org/10.1016/j.surfcoat.2019.03.055*.